

PAPER

Light-trapping structure based on ultra-thin GaAs solar cell

To cite this article: Y S Peng and S F Gong 2020 *J. Phys. D: Appl. Phys.* **53** 495107

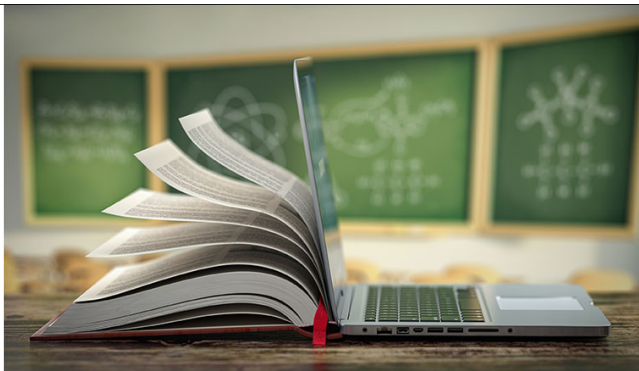
View the [article online](#) for updates and enhancements.



The Electrochemical Society
Advancing solid state & electrochemical science & technology
2021 Virtual Education

Fundamentals of Electrochemistry:
Basic Theory and Kinetic Methods
Instructed by: **Dr. James Noël**
Sun, Sept 19 & Mon, Sept 20 at 12h–15h ET

Register early and save!



Light-trapping structure based on ultra-thin GaAs solar cell

Y S Peng  and S F Gong

College of Information Engineering, Zhejiang University of Technology, Hangzhou 310023, People's Republic of China

E-mail: gongsf@zjut.edu.cn

Received 3 February 2020, revised 20 August 2020

Accepted for publication 1 September 2020

Published 6 October 2020



CrossMark

Abstract

It is well-known that the light-trapping effect is very important for improving cell efficiency and reducing material cost. Certain kinds of light-trapping schemes have been explored and applied to thin-film cells, especially to Si-based thin-film solar cells. This is considered less attractive in GaAs thin film cells, due to the fact that GaAs has a high absorption coefficient, a direct bandgap and suffers from strong surface recombination. In this paper, we describe the development of a highly efficient light-trapping structure utilizing periodically patterned front and back dielectric nanopyramid arrays keeping a completely flat GaAs active layer. It was found that our proposed structure was superior for ultra-thin active layers. The optimized structure yielded a photocurrent density of 20.94 mA cm^{-2} with an active layer thickness of $0.1 \mu\text{m}$, which by far exceeded the reference cell photocurrent of 15.31 mA cm^{-2} with an equivalent thickness. These results are very significant for directing research into the light trapping and cost reduction of thin-film GaAs solar cells.

Keywords: nanopyramid array, GaAs solar cell, light trapping, absorption enhancement

(Some figures may appear in colour only in the online journal)

1. Introduction

GaAs solar cells have already received attention due to the fact that GaAs material has several peculiarities such as a direct bandgap, a high carrier mobility rate and a low temperature coefficient, etc [1, 2]. Compared to silicon solar cells, however, the high cost hinders practical large-scale terrestrial applications [3, 4]. Numerous methods have been explored to increase the cost-effectiveness of GaAs solar cells while maintaining a high conversion efficiency. Among the various methods, the most feasible method is to thin down the thickness of the GaAs active layer [5, 6]. However, by doing so, the absorption efficiency for most of the available spectral range in the active layer is significantly reduced, due to limited absorption. Therefore, in order to increase the absorption of photons, various light-trapping mechanisms have been proposed.

A kind of very attractive solar cell light-trapping mechanism has been proposed, whereby the active layer is patterned with an array of nanostructures on the top or bottom of the active layer, where the active layer is part of the array, such as nanolines [7, 8], nanopores [9], vertical nanocones

[10], nanopyramids [11], and so on. This architecture traps light through strong diffracted and propagated waveguide modes at the interface between the semiconductor and the light-trapping structures, which result in photon absorption enhancement. However, the literature mentioned above mainly focuses just on crystalline silicon thin-film solar cells, which have not yet been effectively applied to GaAs solar cells serving as light-trapping structures. Because GaAs has a much higher surface recombination velocity, if the active layer is directly patterned into an array of nanostructures, the surface damage will lead to a significant drop in efficiency [12, 13]. Recently, however, numerous light-trapping approaches for GaAs solar cells have been explored [14–19], such as photonic crystal arrays combined with distributed Bragg reflection (DBR) [16], and plasmon enhancement effects [18, 19]. However, almost all of the literature mentioned above focuses on light-trapping structures either on the top or the bottom of the active layer. There is little research into combination structures and their correlation with the enhancement of thin-film solar cell photon absorption. Recently, Prathap Pathi *et al* [20] reported an

ultrathin crystalline silicon solar cell that was remarkably improved by the combined effect of two-sided dielectric nanocones, which patterned a light-trapping structure on dielectric materials instead of the active layer, leading to a J_{sc} of 29.5 mA cm^{-2} for $3.6 \text{ }\mu\text{m}$ thick poly-Si. There is a potential for $20 \text{ }\mu\text{m}$ thick cells to provide 30 mA cm^{-2} of photocurrent and an efficiency higher than 20%. However, this light-trapping nanostructure has not yet been applied to GaAs solar cells. Therefore, determining the optimal light-trapping nanostructures for GaAs solar cells is still an open issue, which we will address in this article.

In this paper, we develop a similar alternative light-trapping architecture utilizing periodic nanopyramid arrays of dielectric materials both on the front and back of the active layer combined with a silver back reflector.

2. Structure and approach

Our designed solar cell architecture is shown in figure 1(a), including a square photonic crystal array of dielectric TiO_2 nanopyrramids with a height of h_1 and pitch of a on the top of a flat GaAs active layer, followed by lower TiO_2 nanopyramid arrays with height h_2 and the same pitch a and a back reflector. To start out, we assume the back reflector is made of a perfect electric conductor (PEC) [21], and then we will consider a more realistic silver back reflector with metal loss.

TiO_2 was chosen as the dielectric layer, because it has the dual characteristics of passivating the GaAs surface and transporting electrons.

The top nanopyramid array diffracts the incident light into the active layer. Due to the gradual transition of the refractive index from air to the dielectric, impedance mismatch and reflection loss are reduced. The bottom photonic crystal array is very effective for the diffraction of long-wavelength photons reaching the back of the active layer.

We start out by designing and optimizing the front and rear nanopyrramids' photon crystal arrays utilizing the rigorous coupled wave analysis (RCWA) method to obtain absorption, reflection and transmission in the active layer [22, 23]. In this paper, experimentally measured wavelength-dependent complex dielectric functions $\varepsilon(\lambda)$ of GaAs [24], TiO_2 [25], Si_3N_4 [26] and Ag [27] are utilized.

The RCWA method expresses the electromagnetic field as the sum of coupled waves. The periodic permittivity function is expressed using Fourier harmonics. Each coupled wave is related to a Fourier harmonic, so that the entire vector Maxwell equation can be solved in the Fourier domain. To solve the simulation equation, the structure is considered to be a multilayer periodic structure, which is decomposed into a stack of layers with vertically homogeneous regions. A multi-layer structure is designed in the vertical direction (z direction) and has a periodic structure in the x - y direction. Considering the periodic boundary conditions, we only use a single period in the x - y dimension. From the simulation, the total reflectance ($R(\lambda)$) and transmission ($T(\lambda)$) for each incoming wavelength can be obtained. The absorption at each wavelength is then $A(\lambda) = 1 - R(\lambda) - T(\lambda)$. The calculated

total absorption in the GaAs layer is weighted by the air mass (AM 1.5) solar spectrum and integrated from $0.4 \text{ }\mu\text{m}$ (λ_{\min}) to $0.9 \text{ }\mu\text{m}$ (λ_{\max}) to obtain the average absorption $\langle Aw \rangle$.

$$\langle Aw \rangle = \int_{\lambda_{\min}}^{\lambda_{\max}} A(\lambda) \frac{dI}{d\lambda} d\lambda \quad (1)$$

where λ is the incident wavelength, and $\frac{dI}{d\lambda}$ is the incident solar spectrum [28]. Here, it should be noted that the Fourier harmonic number H plays an important role in determining the accuracy of the simulation result, because it is used to expand the refractive index and field in the Fourier space. The greater the value of H used, the more accurate the simulation results will be, but at the expense of more simulation time and memory. Therefore, we needed to conduct a convergence study on a number of different harmonics to see the changes in the simulation results. Figure 1(b) shows the absorption convergence plot for different H values. It is found that the absorption becomes almost stable for values of H equal to or more than five, thus in our simulation, a H of five is used.

We then compare the performance of our structure to both the reference cell with a planar anti-reflector combined with a PEC reflector and the Yablonovitch limit absorption. For the case through the active layer without considering reflection losses and perfect light trapping, the absorption spectrum in an active layer with thickness t is given by the Yablonovitch limit [29, 30]

$$A_Y = 1 - \frac{1}{1 + 4n^2\alpha t} \quad (2)$$

where α is the absorption coefficient and n is the real part of the refractive index.

Finally, we characterized and compared the short-circuit current density (J_{sc}) among nanopyramid arrays, with reference to the light-trapping structure and the Yablonovitch limit of an ultrathin GaAs active layer.

3. Results and discussion

We performed a systematic set of optimizations for all parameters with the purpose of achieving maximum photon absorption by maximizing antireflection at the front surface and minimizing transmission at the back surface over the solar spectrum (0.4 – $0.9 \text{ }\mu\text{m}$) for a GaAs cell.

The large index mismatch between the dielectric material and the air causes significant reflection losses for flat structures. This can be reduced using ergonomic tapered nanostructures which grade the refractive index from dielectric material to the air value. Therefore, to achieve effective antireflection, a high aspect ratio (h_1/a) is preferred to provide a smooth index transition from the air to the dielectric material [21]. To start with, we demonstrate an optimization study of only the upper nanopyramid array, without the rear reflector. The optimization includes the array pitch (a) and the nanopyramid height (h_1), where these two parameters affect each other. Therefore, we have used a contour map to show the optimization of the nanopyramid structure. The total absorption $\langle Aw \rangle$ of a GaAs

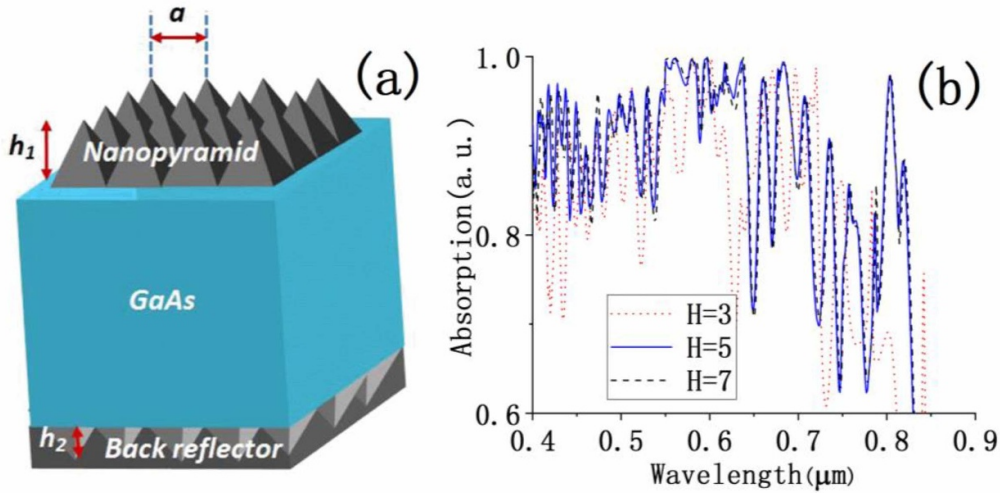


Figure 1. (a) A GaAs solar cell architecture with double-sided dielectric nanopillar arrays combined with a back reflector. (b) Convergence of the calculated absorption as a function of the harmonic number H .

active layer with a $0.7 \mu\text{m}$ thickness is a function of a and h_1 , as shown in figure 2(a). Obviously, the total absorption has a strong inter-dependence on the nanopillar pitch and height.

The largest absorption occurs with a pitch ranging from $0.5\text{--}0.65 \mu\text{m}$ and a height range of $3.5\text{--}5 \mu\text{m}$; the highest weight absorption $\langle Aw \rangle$ of 0.55 is obtained with a pitch and height of $0.55 \mu\text{m}$ and $4.5 \mu\text{m}$, respectively. From figure 2(a), it can be found that this structure with only the front light-trapping structure exhibits a good tolerance for high photon absorption efficiency with regard to variation in the parameters of a and h_1 . For example, a nanopillar pitch of $0.55 \mu\text{m}$ can be coupled with a front array height of $3.5\text{--}5.0 \mu\text{m}$. Therefore, it is possible to manufacture our proposed device utilizing the available semiconductor processing techniques and this still has the ability to provide optimal results.

Figure 2(b) exhibits the reflection spectrum for an optimal nanopillar pitch and height of 0.55 and $4.5 \mu\text{m}$. Reflection of less than 20% is clearly demonstrated and the average reflection level is below 10% in the wavelength range from $0.4\text{--}0.85 \mu\text{m}$. Nanopillar arrays can suppress reflection, due to the nanopillars' average graded index from air to the active layer, because their cross-section gradually increases from zero to the maximum at the planar film surface. The reflection suppression is very broadband, since the index-matching is largely independent of wavelength [21].

Next, we kept the upper nanopillar array optimal geometry fixed, and then calculated the average absorption $\langle Aw \rangle$ as a function of the height of the back side of the nanopillar construction. In our simulation, for computational convenience, the same pitch is chosen for the front and rear nanopillar arrays. The optimal height (h_2) of the back nanopillar is around $0.48 \mu\text{m}$, which is shown in figure 3.

In order to determine whether the optimal parameters will vary with the thickness of the active layer, we performed systematic optimization calculations for the active layer in the thickness range from 0.1 to $1 \mu\text{m}$. It was found that for different active layer thicknesses, the optimal photonic crystal

parameters corresponding to the maximum absorption were almost the same, which is consistent with references [20, 21].

The optimal parameters are summarized in table 1. Figure 4 shows the absorption spectrum for a GaAs solar cell with an active layer $0.1 \mu\text{m}$ thick, corresponding to the optimal nanopillar array parameters.

From figure 4, many diffraction peaks can be observed within the entire spectrum of interest and these result in an overall absorption efficiency enhancement. The diffraction mechanism can be expressed as follows. With an active layer thickness of t , all resonances should pick up a round trip phase variance of $2m\pi$, so that $k_z = m\pi/t$. The wavelength of the diffraction resonant mode is given by [31]

$$\lambda = \frac{2\pi n(\lambda)}{\sqrt{G_x^2 + G_y^2 + (m\pi/t)^2}} \quad (3)$$

where m is an integer, $n(\lambda)$ is the refractive index of GaAs, and G_x and G_y are the components of the reciprocal lattice vectors ($G_x = i(2\pi/a)$ and $G_y = j(2\pi/a)$, a is the array pitch). The diffraction resonances occurring for integer values of i, j , and m satisfy equation (3), exhibiting absorption peaks in the range of interesting wavelengths. The peaks overlap and form an overall absorption enhancement. Our simulations show that diffraction resonance is most effective, and the highest absorption efficiency is obtained, when a is equal to $0.55 \mu\text{m}$.

In order to better understand the absorption enhancement effect in the proposed light-trapping structure, we have compared it to a reference cell (with a frontal Si_3N_4 anti-reflection layer and a rear PEC reflector) and the Yablonoitch limit. The calculated absorption spectra with different light-trapping structures are shown in figure 5, keeping an ultrathin active layer of $0.1 \mu\text{m}$ thickness.

Starting from the case with a front anti-reflection structure only as shown in figure 5(a), it can be observed that the proposed structure exhibits a significantly high absorption enhancement in the entire wavelength range of $0.4\text{--}0.85 \mu\text{m}$. In particular, when the wavelength is greater than $0.55 \mu\text{m}$, the

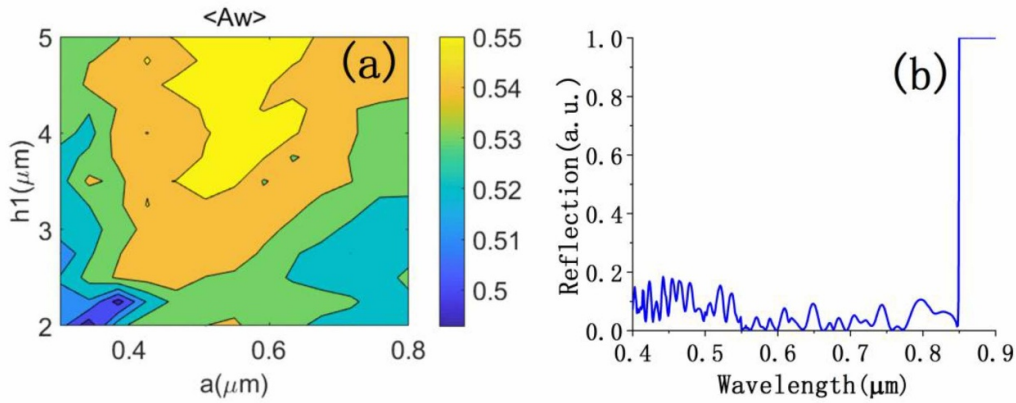


Figure 2. (a) The contour map of absorption as a function of h_1 and a for an active layer of $0.7 \mu\text{m}$ thickness; (b) The reflection spectrum with an optimal frontal nanopyramid array.

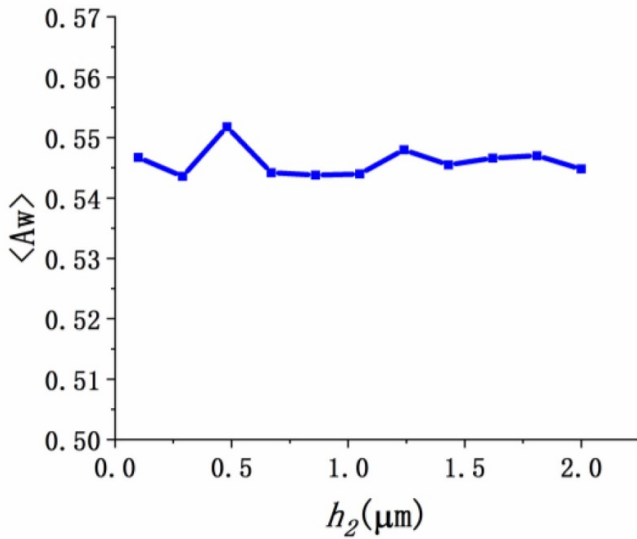


Figure 3. Calculated $\langle A_w \rangle$ as a function of h_2 for a $0.7 \mu\text{m}$ thick active layer.

Table 1. Summary of the optimal parameters of nanopyramid arrays.

No.	arameter	Value(μm)
1	Array pitch (a)	0.55
2	Upper nanopyramid height (h_1)	4.5
3	Bottom nanopyramid height (h_2)	0.48

absorption for the optimal structure greatly exceeds that for the reference structure, and many diffraction absorption peaks are clearly observed. This shows that the front nanopyramid array is particularly advantageous in reducing reflectance loss and coupling long wavelength photons into the active layer.

Alternatively, when the back reflector structure only is added to the flat active layer, the absorption spectra are as shown in figure 5(b). The rear nanopyramid array affects only photons that reach the back reflector without being absorbed in the active layer and generates enhanced absorption. For the reference cell, one absorption peak is observed at a

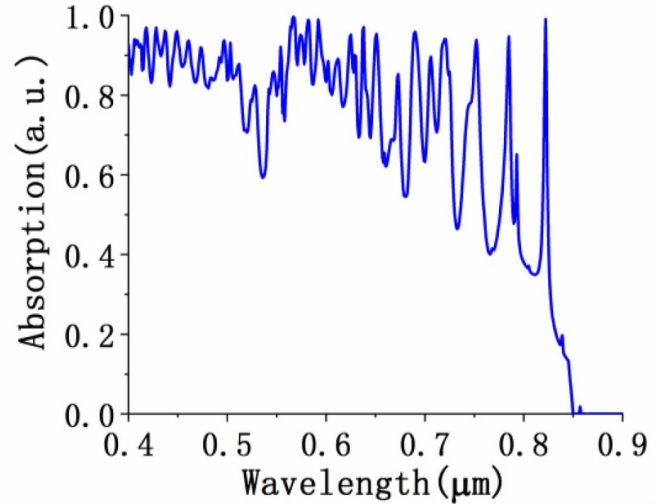


Figure 4. The absorption spectrum for a $0.1 \mu\text{m}$ thick active layer with an optimal light-trapping structure.

short wavelength of around $0.55 \mu\text{m}$, where a waveguide effect occurs in the plane of the structure. For nanopyramid structure cells, in the long wavelength regime of $0.6\text{--}0.85 \mu\text{m}$, the absorption is significantly enhanced and exhibits several diffract peaks due to the diffraction effect from the back nanopyramid arrays.

The optimal front- and rear-nanopyramid arrays were combined and generated a high absorption enhancement over a wide wavelength regime (figure 5(c)), which is shown by red line in the figure. One can observe that the absorption is very close to the Yablonoitch limit in the long wavelength regime of $0.55\text{--}0.85 \mu\text{m}$, and the absorption exceeds the Yablonoitch limit at some specific wavelengths where waveguiding occurs in the plane of the structure.

Next, it is necessary to study the absorption enhancement as a function of GaAs active layer thickness for different light-trapping architectures. In order to clarify the relationship among different structures, an integration absorption enhancement (IAE) is defined as the total amount of absorbed solar photons divided by the total amount of incoming solar

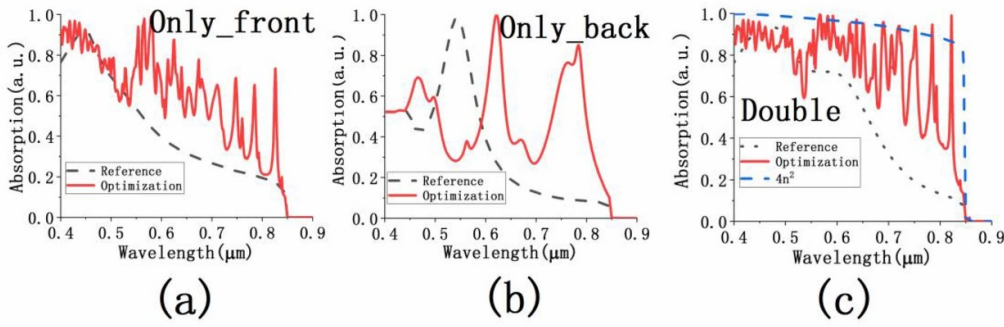


Figure 5. Comparison of absorption spectra for different light-trapping configurations with a 0.1 μm thick active layer are shown in (a) the front cell only, (b) the back cell only, and (c) both the optimal and typical cells as well as the Yablonovitch limit.

photons. The mathematical expression is shown as follows in equation (4).

$$IAE = \frac{\int_{\lambda_{min}}^{\lambda_{max}} A(\lambda) \frac{dI}{d\lambda} d\lambda}{\int_{\lambda_{min}}^{\lambda_{max}} \frac{dI}{d\lambda} d\lambda} \times 100\% \quad (4)$$

Figure 6(a) shows the IAE as a function of active layer thickness for the optimal and reference cells with different light-trapping structures as well as for the Yablonovitch limit. For the solar cell with optimal nanopyramid arrays, the optimal a , h_1 and h_2 are 0.55 μm, 4.5 μm and 0.48 μm, respectively; for reference solar cells, the optimal anti-reflector Si₃N₄ layer thickness is 60 nm.

As expected, the benefit of light trapping is more pronounced for thinner films. It can be observed that the IAE nearly saturates when the active layer thickness is approximately 3 μm, corresponding to the thickness that almost fully absorbs the incident light and that does not require rear light trapping, whereas the IAE drops significantly as the active layer thickness is reduced to less than 1 μm. For example, at 0.1 μm, the IAE is around 68.85% for the cell with the optimal nanopyramid arrays and is 26.8% lower than its saturation value of 87.30% at 3 μm. This significant reduction indicates that the light-trapping structure is particularly important for improving the photon absorption of the ultra-thin active layer.

For our designed structure, the front nanoarray is more effective compared to the back nanoarray. The IAE values are around 58% and 45% for the front-only and back-only nanoarrays with an active layer 0.1 μm thick, respectively. A substantial absorption enhancement is exhibited as the active layer thickness increases; an IAE saturation value of 87.01% is obtained for the front-only nanoarray, which significantly exceeds the back-only nanoarray's benefit with a saturation IAE of 59.09%.

For the reference solar cells, the IAE exhibits a similar variation in trend to our design cells. The major absorption enhancement also comes from the frontal antireflection effect. However, the highest-performance architecture is based on our proposed solar cells with their optimal light-trapping structures, especially for cells with ultra-thin active layers. For example, for the optimized and reference cells with an active layer thickness of 0.1 μm, the IAE values are 68.85% and

53.83%, respectively. The absolute increase is 15.02%, and the relative increase is around 27.90%.

In addition, the reference cell exhibits almost the same absorption enhancement as our optimal cell when the active layer thickness is greater than 1 μm. For example, for an active layer 2 μm thick, the IAE of the optimal cell is around 87.16%, whereas that of the reference cell is approximately 86.38%. This means that, for ultra-thin solar cells, our structure has advantages over the reference structure, exhibiting a more effective light-trapping function. However, it could also be observed that although our proposed structure was able to achieve a much higher absorption efficiency, this IAE is still below the Yablonovitch limit value of 93.97%, as shown in figure 6(a).

We will now make a comparison of the short-circuit current density (J_{sc}) among solar cells with different light-trapping structures for the same active layer thickness of 0.1 μm, to highlight their comparative performance. It should be noted that the purpose of this study is to demonstrate the optical effect mechanism of nanopyramid array light trapping for solar cells; we will not cover the details of the charge carrier collection and transport properties of the cell. Therefore, it is assumed the internal quantum efficiency (IQE) is equal to one, i.e. the absorption of each incident photon generates an electron-hole pair. The short-circuit current density J_{sc} is a spectrally-integrated quantity, defined as:

$$J_{sc} = \frac{e}{hc} \int_{\lambda_{min}}^{\lambda_{max}} \lambda A(\lambda) IQE(\lambda) \frac{dI}{d\lambda} d\lambda = \frac{e}{hc} \int_{\lambda_{min}}^{\lambda_{max}} \lambda A(\lambda) \frac{dI}{d\lambda} d\lambda \quad (5)$$

Here, $\frac{dI}{d\lambda}$ is the incident solar spectrum, e is the electronic charge, λ is the incident wavelength, h is Planck's constant, c is the speed of light.

The values of J_{sc} for solar cells with different light-trapping structures are shown as figure 6(b). The optimal nanopyramid structure achieves 20.94 mA cm⁻², while the reference cell only achieves 15.31 mA cm⁻². Furthermore, the values of J_{sc} for our optimal 'front-only' and 'back-only' structures are 17.46 and 13.35 mA cm⁻², respectively, outperforming that of the reference structure with a 'front-only' value of 12.22 mA cm⁻² and a 'back-only' value of 9.99 mA cm⁻². However, the J_{sc} is still below 27.62 mA cm⁻², corresponding to the Yablonovitch limit at the equivalent thickness of 0.1 μm.

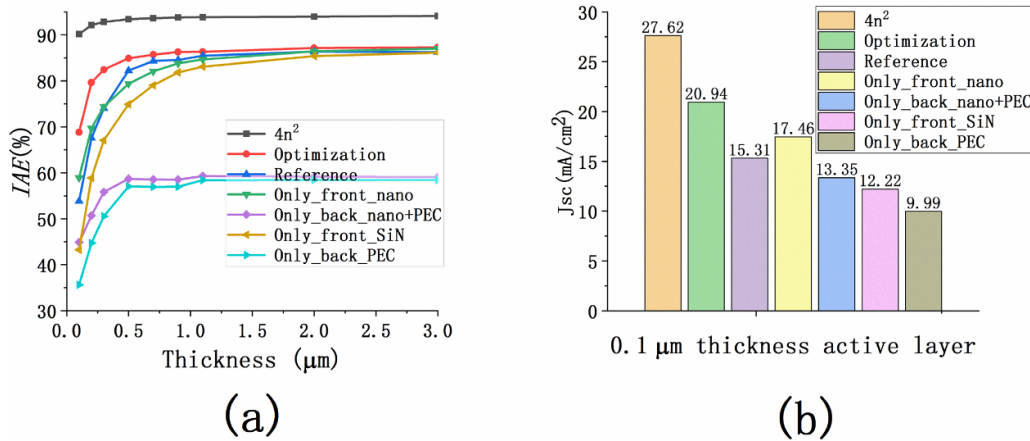


Figure 6. (a) Calculated IAE for different light-trapping constructions as a function of the active layer thickness; (b) J_{sc} of solar cells with a $0.1 \mu\text{m}$ thick active layer for different light-trapping constructions.

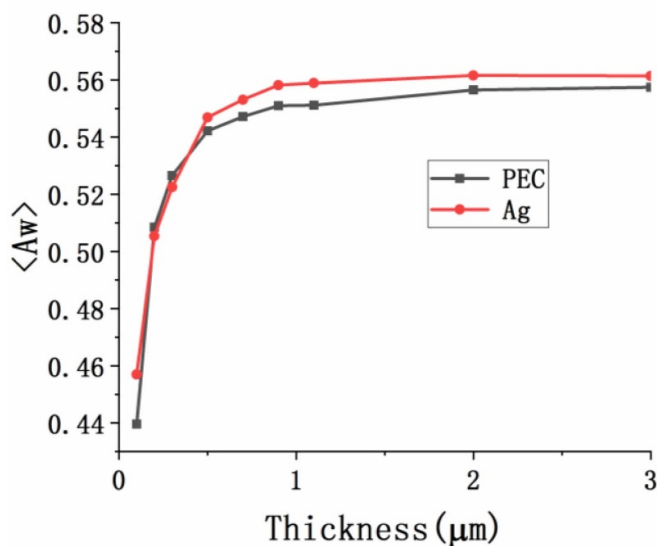


Figure 7. Calculated $\langle A_w \rangle$ as a function of active layer thickness for PEC and Ag back reflectors, respectively.

To characterize the loss of a real back reflector, we replaced the PEC layer by a flat silver layer for the optimized structure. The average absorption $\langle A_w \rangle$ for the PEC was only slightly lower than the silver back reflector by $0.04\text{--}0.017 \text{ W m}^{-2}$, as seen in figure 7, indicating small losses in the silver back reflector.

In addition, when we extended our optimization to include nanopillar arrays made of other dielectric materials such as SiN, we observed similar geometrical configurations and absorption enhancements. Therefore, this strategy has great flexibility for the nanopillar array design regarding the material choice for the front and rear photonic crystal arrays.

Finally, it should be noted that the optimized structure could be fabricated using either the Langmuir–Blodgett (LB) assembly method and reactive ion etching (RIE) or nanoimprint lithography (NIL) of sol-gel-derived TiO₂ layers. The nanopillar array provides an experimentally realistic

strategy for efficiency improvement and cost reduction of GaAs solar cells.

4. Conclusion

In conclusion, we developed a highly efficient light-trapping architecture utilizing periodically patterned front and rear dielectric nanopillar arrays with a completely flat GaAs active layer, ensuring that the absorber layer had completely flat interfaces, which was expected to result in high electronic quality and low carrier recombination, where the front and rear nanopillar arrays were separately optimized. The absorption performance has been compared with both the Yablonovitch limits and the reference planar cell; the results demonstrate that our proposed structure is superior for the ultra-thin active layers. The optimized structure yields a photocurrent of 20.94 mA cm^{-2} and considerably exceeds the reference cell photocurrent of 15.31 mA cm^{-2} with an equivalent thickness of $0.1 \mu\text{m}$. These conclusions are important for directing research into the light trapping and cost reduction of thin-film GaAs solar cells.

Acknowledgments

The authors would like to thank Zhejiang Provincial Department of education for their financial support of this research (Grant Nos. Y201121882 and Y201225406).

ORCID iD

Y S Peng  <https://orcid.org/0000-0002-7426-950X>

References

- [1] Lee S M, Kwong A, Jung D, Faucher J, Biswas R, Shen L, Kang D, Lee M L and Yoon J 2015 High performance ultrathin GaAs solar cells enabled with heterogeneously integrated dielectric periodic nanostructures *ACS Nano* **9** 10356–65

- [2] Green M A, Emery K, Hishikawa Y, Warta W and Dunlop E D 2015 Solar cell efficiency tables (Version 45) *Prog. Photovolt.* **23** 1–9
- [3] Wang X, Khan M R, Gray J L, Alam M A and Lundstrom M S 2013 Design of GaAs solar cells operating close to the Shockley-Queisser limit *IEEE J. Photovolt.* **3** 737–44
- [4] Yablonovitch E, Miller O D and Kurtz S R 2012 The opto-electronic physics that broke the efficiency limit in solar cells presented at the photovoltaic specialists conference *IEEE* **42** 1556–9
- [5] Moon S, Kim K, Kim Y, Heo J and Lee J 2016 Highly efficient single-junction GaAs thin-film solar cell on flexible substrate *Sci. Rep.* **6** 30107
- [6] Vandamme N, Chen H L, Gaucher A, Behaghel B, Lemaître A, Cattoni A, Dupuis C, Bardou N, Guillemoles J F and Collin S 2015 Ultrathin GaAs solar cells with a silver back mirror *IEEE J. Photovolt.* **5** 565–70
- [7] Demesy G and John S 2012 Solar energy trapping with modulated silicon nanowire photonic crystals *J. Appl. Phys.* **112** 074326
- [8] Xu Z, Qiao H, Huangfu H, Li X, Guo J and Wang H 2015 Optical absorption of several nanostructures arrays for silicon solar cells *Opt. Commun.* **356** 526–9
- [9] Han S E and Chen G 2010 Optical absorption enhancement in silicon nanohole arrays for solar photovoltaics *Nano Lett.* **10** 1012–5
- [10] Du Q, Kam C H, Demir H V, Yu H Y and Sun X W 2011 Broadband absorption enhancement in randomly positioned silicon nanowire arrays for solar cell applications *Opt. Lett.* **36** 1713–9
- [11] Haase C and Stiebig H 2007 Thin-film silicon solar cells with efficient periodic light trapping texture *Appl. Phys. Lett.* **91** 061116
- [12] Zeng L, Yi Y, Hong C, Liu J, Feng N, Duan X, Kimerling L C and Alamariu B A 2006 Efficiency enhancement in Si solar cells by textured photonic crystal back reflector *Appl. Phys. Lett.* **89** 111111
- [13] Priolo F, Gregorkiewicz T, Galli M and Krauss T F 2014 Silicon nanostructures for photonics and photovoltaics *Nat. Nanotechnol.* **9** 19–32
- [14] Honsberg C B and Barnett A M 1991 Light trapping in thin film GaAs solar cells *Conf. Record 22nd IEEE Photovoltaic Specialists Conf.* (Las Vegas, NV) pp 262–7
- [15] Miller O D, Yablonovitch E and Kurtz S R 2012 Strong internal and external luminescence as solar cells approach the Shockley–Queisser limit *IEEE J. Photovolt.* **2** 303–11
- [16] Gupta N D and Janyani V 2019 Analysis of photonic crystal diffraction grating based light trapping structure for GaAs solar cell *IETE J. Res.* **1**–12
- [17] Xiao J, Fang H, Su R, Ezheng Li K, Song J, Rauss T F K, Li J and Artins E R M 2018 Paths to light trapping in thin film GaAs solar cells *Opt. Express* **26** 341–51
- [18] Singh G and Verma S S 2019 Plasmon enhanced light trapping in thin film GaAs solar cells by Alnanoparticle array *Phys. Lett. A* **383** 1526–30
- [19] Zhu S-Q *et al* 2019 Enhancement in power conversion efficiency of GaAs solar cells by utilizing gold nanostar film for light-trapping *Frontiers Chem.* **7** 137
- [20] Pathi P, Peer A and Biswas R 2017 Nano-photonics structures for light trapping in ultra-thin crystalline silicon solar cells *Nanomaterials* **7** 1–16
- [21] Wang K X, Yu Z, Liu V, Cui Y and Fan S 2012 Absorption enhancement in ultrathin crystalline silicon solar cells with antireflection and light-trapping nanocone gratings *Nano Lett.* **12** 1616–9
- [22] Li L 1997 New formulation of the Fourier modal method for crossed surface-relief gratings *J. Opt. Soc. Am. A* **4** 2758–67
- [23] Popov E and Nevière M 2001 Maxwell equations in Fourier space: fast-converging formulation for diffraction by arbitrary shaped, periodic, anisotropic media *J. Opt. Soc. Am. A* **18** 2886–94
- [24] Aspnes D E, Kelso S M, Logan R A and Bhat R 1986 Optical properties of Al_xGa_{1-x}As *J. Appl. Phys.* **60** 754–67
- [25] Devore J R 1951 Refractive indices of rutile and sphalerite *J. Opt. Soc. Am.* **41** 416–9
- [26] Philipp H R 1973 Optical properties of silicon nitride *J. Electrochim. Soc.* **120** 295–300
- [27] Johnson P B and Christy R W 1972 Optical constants of the noble metals *Phys. Rev. B* **6** 4370–9
- [28] ASTM G173-03 2005 *Standard Tables for Reference Solar Spectral Irradiances* (West Conshohocken, PA: ASTM International)
- [29] Yablonovitch E and Cody G D 1982 Intensity enhancement in textured optical sheets for solar cells *IEEE Trans. Electron Devices* **ED-29** 300–5
- [30] Green M A 2002 Lambertian light trapping in textured solar cells and light-emitting diodes: analytical solutions *Prog. Photovolt.* **10** 235–41
- [31] Gupta N and Janyani V 2016 Design and optimization of photonic crystal diffraction grating based efficient light trapping structure for GaAs thin film solar cell *J. Nanoelectron. Optoelectron.* **11** 407–15